HHS Public Access

Author manuscript

Curr Biol. Author manuscript; available in PMC 2020 October 21.

Published in final edited form as:

Curr Biol. 2019 October 21; 29(20): 3478–3487.e4. doi:10.1016/j.cub.2019.08.063.

Neuropsin (OPN5) mediates local light-dependent induction of circadian clock genes and circadian photoentrainment in exposed murine skin

Ethan D. Buhr[1,7,8,*], **Shruti Vemaraju**[3,4,5,7], **Nicolás Diaz**[1], **Richard A. Lang**[3,4,5,6,*], **Russell N. Van Gelder**[1,2]

[1]Department of Ophthalmology, University of Washington School of Medicine, 750 Republican St, Seattle, WA 98109, USA

[2]Department of Biological Structure and Department of Pathology, University of Washington School of Medicine, 750 Republican St, Seattle, WA 98109, USA

[3]Center for Chronobiology, University of Cincinnati, College of Medicine, 3333 Burnet Ave, Cincinnati, OH 45229-3039, USA

[4]The Visual Systems Group, Abrahamson Pediatric Eye Institute, University of Cincinnati, College of Medicine, 3333 Burnet Ave, Cincinnati, OH 45229-3039, USA

[5]Division of Pediatric Ophthalmology, Cincinnati Children's Hospital Medical Center, University of Cincinnati, College of Medicine, 3333 Burnet Ave, Cincinnati, OH 45229-3039, USA

[6]Department of Ophthalmology, University of Cincinnati, College of Medicine, 3333 Burnet Ave, Cincinnati, OH 45229-3039, USA

[7]These authors contributed equally

[8]Lead Contact

SUMMARY

Nearly all mammalian tissues have functional, autonomous circadian clocks, which free-run with non-24-hour periods and must be synchronized (entrained) to the 24-hour day. This entrainment mechanism is thought to be hierarchical, with photic input to the retina entraining the master circadian clock in the suprachiasmatic nuclei (SCN), and the SCN in turn synchronizing peripheral tissues via endocrine mechanisms. Here we assess the function of a population of melanocyte precursor cells in hair and vibrissal follicles that express the photopigment neuropsin (OPN5). Organotypic cultures of murine outer ear and vibrissal skin entrain to a light-dark cycle *ex vivo*, requiring *cis*-retinal chromophore and *Opn5* gene function. Short-wavelength light strongly phase

[*]Corresponding authors: Ethan D. Buhr, PhD, Department of Ophthalmology, Campus Box 358058, University of Washington School of Medicine, 750 Republican St, Seattle, WA 98109, USA, buhre@uw.edu; Richard Lang, PhD, Divisions of Ophthalmology and Developmental Biology, Cincinnati Children's Hospital Medical Center, University of Cincinnati, 3333 Burnet Ave., Cincinnati, OH 45229-3039, USA, richard.lang@cchmc.org.

Author Contributions

E.D.B, S.V., R.A.L., and R.N.V.G designed research and supervised the project. E.D.B., S.V., and N.D. performed research. E.D.B, S.V., R.A.L., and R.N.V.G. wrote the manuscript.

Declaration of Interests

The authors declare no competing interests.

shifts skin circadian rhythms *ex vivo* via an *Opn5*-dependent mechanism. *In vivo*, the normal amplitude of *Period* mRNA expression in outer ear skin is dependent on both the light-dark cycle and on *Opn5* function. In *Opn4*$^{-/-}$; *Pde6b*$^{rd1/rd1}$ mice that cannot behaviorally entrain to light-dark cycles, the phase of skin clock gene expression remains synchronized to the light-dark cycle even as other peripheral clocks remain phase-locked to the free-running behavioral rhythm. Taken together, these results demonstrate the presence of a direct photic circadian entrainment pathway and direct light-response elements for clock genes in murine skin, similar to pathways previously described for invertebrates and certain non-mammalian vertebrates.

Keywords

circadian rhythms; opsin; opn5; neuropsin; entrainment; skin

INTRODUCTION

Peripheral tissues of mammals can maintain circadian rhythms of gene expression for months when cultured *in vitro* [1], but synchronization of these peripheral clocks to each other and to the 24-hour light-dark (LD) cycle *in vivo* is thought to be mediated through signals emanating from the SCN [2]. An alternate mechanism, whereby the light cycle directly entrains peripheral oscillators through local photopigments, is utilized by invertebrates such as *Drosophila* [3] and non-mammalian vertebrates such as zebrafish [4]. To date, however, direct light entrainment of non-ocular tissues in mammals has not been demonstrated [5, 6].

Expression of opsin family members in skin has been reported in several organisms including mammals [7–11]. The functions of these opsins are still being determined and may be diverse. Light exposure causes chromatophore expansion in *Xenopus* dermal melanocytes, and this is mediated by melanopsin (OPN4) [9, 12, 13]. Similarly, opsin-mediated photoreception is thought to cause chromatophore expansion in octopus skin [8]. Short-wavelength light has been shown to induce a local, delayed electrical response from the skin of the outer ear in mammals, although the photoreceptor responsible for this effect is unknown [14].

Neuropsin (OPN5) is an opsin family member known to function as a photopigment responsive to wavelengths in the near-UV (λmax = 380 nm) [15, 16]. OPN5 is expressed in paraventricular organ neurons in birds where it is suggested to mediate photoreception relating to seasonality [17, 18]. In mammals, OPN5 is required for photoentrainment of the local circadian oscillator in the murine retina and cornea [19]. Previous studies have found *Opn5* expression in the outer ear skin of mice [16], but its function in this tissue is unknown. Here we show that short-wavelength light can directy photoentrain circadian rhythms in murine skin, and induce clock gene expression both *in vitro* and *in vivo* through an *Opn5*-dependent mechanism, suggesting that mammals may utilize local photic cues in peripheral tissue for circadian entrainment.

RESULTS

Localization of OPN5 Expressing Cells in Dermal Melanocytes

To analyze the expression of OPN5 in skin we utilized a Cre-recombinase knock-in allele of *Opn5* (*Opn5*^{cre}, Figure S1), crossed to the tdTomato-expressing *Ai14* reporter (as no validated anti-OPN5 antibody has been reported to date, and published antibodies show non-specific staining in knockout strains [19]). Histologic analysis of ear (pinna) and vibrissal pad skin from P8 mice revealed reporter expression in two populations of cells: a diffusely distributed, minor population under the epidermis (Figure 1B, dashed line), and a more numerous population in the base of hair follicles (Figure 1A–C). These clusters of *Opn5*-expressing cells co-labelled for c-KIT, MITF, DCT (TRP-2), β-catenin, and LEF1 (Figure 1D–I). These represent markers for melanocyte progenitor cells within the hair bulb [20–25]. However, it should be noted that *Opn5*$^{-/-}$ mice do not exhibit overt hyperpigmentation or albinism. In adult mice, a PCR-based survey confirmed *Opn5* expression in retina, ear pinna, and nose skin vibrissae (Figure 1J). *Opn5* transcript was not observed in the ventral or dorsal skin of the forepaw, nor in pituitary or liver. Assessment of skin from adult ear pinnae from *Opn5*^{cre}*; Ai14* mice showed an expression pattern like that observed in P8 mice with positive cells within the hair follicle base (Figure 1K). These data indicate that the predominant population of *Opn5* expressing cells in pinna and vibrissal pad resides within the hair and vibrissal follicles.

We also analyzed the level of transcription of other opsins in various regions of adult mouse skin. *Opn5* expression was observed in skin of the dorsal back and tail in addition to the ear pinnae and vibrissae (Figure S2). *Opn2* (rhodopsin) was also detected in the vibrissal pad and dorsal skin, similar to previous reports [11, 26]. *Opn4*, *Opn3*, and *Opn1sw* were not detected at levels above baseline (liver) in any skin area (Figure S2). *Opn3* was qualitatively observed in in most tissues as assayed by presence of correct amplicon size using gel electrophoresis.

Ex vivo Photoentrainment of Skin Circadian Clocks

Previously we reported the absence of photoentrainment in cultured pinna tissue from *Per2*^{Luc} mice [27]. This could indicate a lack of sufficiency for *Opn5* in photoentrainment of ear skin. However, these studies were performed in the absence of exogenous chromophore, which may be required for production of functional photopigment. Exogenous retinaldehyde is necessary to elicit light responses in tissue culture experiments using *Xenopus* melanocytes [12] as well as mammalian cells transfected with human *Opn5* or *Opn4* [28, 29]. Thus, we attempted *ex vivo* photoentrainment of outer ear cultures supplemented with exogenous 9-*cis*-retinaldehyde or *all-trans*-retinaldehyde. Dissected outer ears (pinnae) of *Per2*^{Luc} mice were bisected along the cartilage and each pinna half was cultured separately. The two cultures were then exposed to oppositely phased (referred to as 0° and 180°) 10 h light: 14 h dark cycles for 5 full cycles with or without 10 μM 9-*cis*-retinal. The tissues were then maintained in constant darkness to determine the circadian phase of the *Per2*^{Luc} reporter. Without exogenous retinaldehyde, pinna cultures failed to photoentrain (Figure 2A), corroborating earlier findings [27]. However, in the presence of 9-*cis*-retinal, pinna cultures adopted antiphase *Per2*^{Luc} luminescence rhythms (Figure 2B and J). An assessment

of photoentrainment in the vibrissal pad (3 vibrissal follicles including surrounding fat, dermis, and epidermis) similarly showed the 0° and 180° cultures adopting antiphase *Per2*^{Luc} rhythms but only in the presence of 9-*cis*-retinal (Figure 2D, E, J). When incubated in the presence of *all-trans*-retinal, ear pinna cultures did not exhibit photoentrainment (Figure S3). This is perhaps due to an inability of mammalian OPN5 to bind to retinaldehyde in its *all-trans* state [30]. These data indicate that skin of the pinna and vibrissal pad photoentrain their circadian clocks *ex vivo*.

To determine whether OPN5 was required for *ex vivo* photoentrainment in pinnae and vibrissae, we tested tissues from *Opn5*$^{-/-}$ mice under identical conditions to the wild-type experiments. Neither cultures of pinnae nor vibrissal pads of *Opn5*$^{-/-}$ mice displayed photoentrainment *ex vivo*, even in the presence of 9-*cis*-retinal (Figure 2C, F, J). Wild-type tissues in which *Opn5* was undetectable by RT-PCR, including the pituitary and liver, were not photoentrainable *ex vivo* either with or without 9-*cis*-retinal (Figure 2G, H, I, J). Thus, the dermal tissues of the outer ear and macrovibrissal pad contain photoentrainable circadian clocks that require OPN5 and retinaldehyde chromophore, suggesting that this opsin is functioning as a photopigment in these tissues.

When vertebrate circadian systems undergo a phase shift, a common feature is the photic induction of genes of the *Per* family. In mammals, acute light causes a phase-dependent induction of *Per1* and *Per2* in the SCN [31–33]. To further evaluate the direct effect of light on the circadian clock in mouse skin, we measured light induction of *Per* genes in pinnae *ex vivo*. Tissues from *Per2*^{Luc} mice were held in darkness for at least 36 hours before exposure to a 90 min light pulse from a violet light-emitting diode (peak λ = 415 nm, 2 x 10^{14} photons cm^{-2} s^{-1}) at times across a circadian cycle based on the phase of *Per2*^{Luc} luminescence. Both *Per2* and *Per1* mRNA were strongly induced by the violet light, and the response was gated by the phase of the circadian clock (Figure 3A). Similar to SCN clock phase-dependent behavioral responses to light [34], we observed a “dead zone” during the times of day when the tissue would have been in the light phase of an LD cycle (subjective day), during which the bright violet light elicited no response of the *Per* genes. However, at times nearing the light-to-dark transition (dusk) and into the subjective night, both *Per* genes responded robustly to light (Figure 3A). *In vivo*, violet light administered to mice at circadian time (CT) 13 elicited strong induction of *Per1* and *Per2* transcripts, which was abrogated in *Opn5*$^{-/-}$ mice (Figure 3B). These results suggest photic induction of *Per1* and *Per2* in skin is gated by the circadian clock as has been described in the SCN [31, 32], and that OPN5 is serving as photoreceptor for this induction.

Light-induced phase shifts of *Per2*^{Luc} luminescence rhythms in cultured pinnae displayed a similar pattern of sensitivity during the subjective night, with a ‘Type 0’ strong resetting waveform (Figure 3C) [35]. To ascertain the spectral sensitivity of the phase shifting effect we used light pulses of equal photon flux (2 x 10^{14} photons cm^{-2} s^{-1}) of 475-nm (blue) and 525-nm (green) light. A similar phase-dependent response, but of reduced magnitude was observed for 475-nm light, while there was no observable photic response during the subjective night to 525-nm light (Figure 3C). Violet light pulses (415 nm) as given in Figure 3C were not sufficient to elicit phase shifts from cultured pinnae from *Opn5*$^{-/-}$ mice at any phase of the circadian cycle (Figure 3D and E). This analysis shows that *Opn5* is required

for chomophore-dependent photoentrainment of ear skin *ex vivo*, and for circadian-gated light induction of *Per* mRNA. While the spectral sensitivity peak of mammalian OPN5 in in the UVA range [16], we used 415-nm light in the majority of these *ex vivo* experiments to avoid long term exposure of cell culture media and cultured to UV light. To better test the spectral tuning of the photic phase-shifting response we administered phase delaying light pulses (CT 17-19) using 5 wavelengths from 370 nm to 525 nm over a 10,000-fold intensity range for each wavelength (Figure 3F). We confirm that the strongest phase setting effects were observed with 370 nm near-UV with a monotonic decrease in efficacy with increasing wavelength. Analysis of the relative potency of light of different wavelengths results in an action spectrum for circadian phase shifting that is coincident with the reported absorption spectrum for OPN5 [16, 30] (Figure 3G), these data strongly suggest that OPN5 is acting as the primary photoreceptor for circadian entrainment in skin. Importantly, we do not see significant phase shifting activity with light of 475 nm or 525 nm, a wavelength range encompassing maximally sensitivity for melanopsin (Opn4) and rhodopsin (Opn2).

When luminescence from $Per2^{Luc}$ ear cultures was imaged using a cooled charged-coupled device (CCD) camera, areas of strong luminescence appeared around the areas of hair follicles (Figure 3H). The bioluminescence from hair follicles was spatially associated with groups of *Ai14* expressing cells in $Opn5^{Cre};Ai14$ tissue (Figure 3I). When imaged continuously for days the follicles showed robust circadian oscillations, confirming previous reports of strong circadian activity within hair follicles (Video S1, 2 days)[36, 37]. When measured as independent regions of interest from time-lapse images of a cultured ear, the luminescence rhythms of individual hair follicles within a single tissue drift in phase over days in culture, but are returned to a common phase by a 90 minute, 415-nm light pulse (Figure 3J). This suggests that local entrainment of the circadian clock through OPN5 mediates coordination of circadian phase via daily resetting.

In vivo Effects of OPN5 Loss on Skin Circadian Clocks

To determine the extent to which this photoreceptive system functions *in vivo*, we assessed clock gene expression by qPCR in pinnae over a 24-hour time-course of a 12:12 LD cycle or after 36 hours of constant darkness (DD). In wild-type pinnae in LD, *Per1* and *Per2* showed robust mRNA expression amplitude (Figure 4A, B, blue lines). By contrast, $Opn5^{-/-}$ animals in the same LD cycles did not show the same amplitude of clock gene expression. In particular, a large induction of transcript was observed at around clock time 12 in wild-type mice (or dusk) for *Per2*, *Per1*, *Cry2*, and *Dbp*, but this induction was absent in $Opn5^{-/-}$ ear skin (Figure 4A–D). A similar pattern was observed for *Rev-erbα* but with a prolonged high-amplitude expression through the light phase (Figure 4F and L). In constant darkness (DD) the skin of wild-type animals showed reduced amplitudes of the same genes which showed the strong amplitude of expression in LD, and were not statistically different from $Opn5^{-/-}$ tissue (Figure 4G–J and L). Interestingly, the expression of the core clock gene *Bmal1* was unchanged by lighting conditions or genotype (Figure 4E and K). This suggests that the light-induced amplitude enhancement is acting over an already active circadian clock and is not necessary for the function of the core clock itself. Additionally, a noticeable "hump" of expression occurs in *Per2* and *Cry2* in mid-to-late night in $Opn5^{-/-}$ skin, indicating the presence of systemic light cues, in addition to the OPN5-driven light

sensitivity in the early night (Figure 4A and C). An examination of the expression of *Per1* and *Per2* in the liver (Figure 4M, N) shows that the anticipated expression is unchanged in *Opn5* null mice in both LD and DD conditions. This suggests that the action of OPN5 in regulating the amplitude of clock gene expression in ear skin is local to the skin and not a result of decreased central entrainment. Photic modulation of *Per* gene expression has been suggested as a fundamental mechanism for photic entrainment of the SCN clock by the retina [32, 33]. These results reveal a similar strong diurnal induction of clock-related genes in areas of exposed skin.

Photic Entrainment of Skin Clocks *in vivo*.

The currently accepted model for peripheral circadian oscillator entrainment in mammals posits that entrainment cues for peripheral tissues emanate from the photoentrained SCN [6, 38]. The behavior of some peripheral circadian clocks may not be consistent with this model as they are able to synchronize in the absence of a functional SCN [39]. This leaves open the possibility that peripheral opsin expression could substitute for the SCN in providing photoentrainment cues *in vivo*. To assess the relative contributions of central (SCN-dependent) and local phase control of the skin circadian clock, we utilized mice lacking photic input to the SCN, but with intact OPN5 function in skin. Mice that are null for melanopsin ($Opn4^{-/-}$) and have rod and cone degeneration ($Pde6b^{rd1/rd1}$) do not deliver photic entrainment signals to the SCN and "free run" their locomotor activity cycle through light-dark cycles [40]. Thus, there will be days on which the activity phase of $Opn4^{-/-}$; $Pde6b^{rd1/rd1}$ mice has advanced to become exactly opposite of the LD cycle phase [27]. This provides an opportunity to determine whether the ear skin clock is entrained independently by the light-dark cycle or oscillates in phase with the SCN.

After a minimum of 3 weeks' exposure to the 12 hr light: 12 hr dark cycle, wheel running behavior of $Opn4^{-/-}$; $Pde6b^{rd1/rd1}$ mice was recorded and used as an indication of clock phase for the SCN (Figure 5A). We analyzed clock gene expression rhythmicity in two cohorts of mice. In one cohort, activity onset was coincident with lights-on (diurnal-like) (Figure 5A, red boxes) and in the other cohort, activity onset was coincident with lights-off (nocturnal-like) (blue boxes). RT-PCR analysis showed that in both pinna and vibrissal pad, the phases of *Bmal1*, *Per2*, *Per1*, and *Dbp* expression were the same in both cohorts (Figure 5B and C, red and blue traces), indicating synchronization with the LD cycle. In contrast, clock gene expression in the liver and pituitary remained synchronized with behavior and SCN phase (Figure 5D and E). This strongly suggests that the photoreceptors present in the skin are 1.) capable of photoentraining the local circadian clock *in vivo*, and 2.) that these signals are capable of overriding signals from the central circadian pacemaker controlling behavior in the presence of an LD cycle. This result is qualitatively identical to that previously reported for retinal clock gene expression in the same assay, which also utilize *Opn5*-dependent local entrainment mechanisms [27].

DISCUSSION

OPN5 has previously been shown to be expressed in retinal neurons, and to function in the eye to mediate local photoentrainment of the retina's intrinsic circadian clock [16, 19, 41].

Here we show that OPN5 is expressed extraocularly in vibrissal and ear pinna skin, and functions locally in a photoreceptive mechanism to entrain the circadian rhythms of these tissues directly to the external light-dark cycle. Isolated skin is able to synchronize its circadian oscillations to the light-dark cycle *ex vivo*, likely through OPN5-dependent induction of *Per* gene expression. *In vivo*, this local mechanism allows skin rhythms to maintain synchrony with the light-dark cycle even under conditions in which the central oscillator (as represented by locomotor activity) is free-running. OPN5 expression is also necessary for the full amplitude of diurnal rhythmic *Per* gene expression in LD cycles *in vivo*. The requirement in cultured skin for exogenous *cis*-retinaldehyde to demonstrate photosensitivity, and the coincidence of action spectrum and reported absorption spectrum for OPN5 strongly suggests that the skin photoreceptive mechanism utilizes OPN5 as a photopigment. Circadian clocks within mammalian skin control the response to UV light [42, 43], as well as cell cycle progression in hair follicles [36] and keratinocytes [44, 45], and response to physical injury [46, 47]. The current results would suggest that light modulation of these clocks through OPN5 function may significantly influence these physiologies. Further, these results suggest that mammals, like fish [48], amphibians [49], and birds [17, 50] utilize extraocular opsin photopigments for direct, light-dependent regulation of circadian clock function in some peripheral tissues. This challenges the widely-held dogma that peripheral circadian rhythms within mammals are synchronized exclusively by the master SCN circadian pacemaker via ocular photoreception [51, 52], and suggests mammals also use local light sensing in peripheral tissues for this purpose.

The expression of opsins in extra-retinal sites opens important questions about their physiology. In the retina, 11-*cis*-retinaldehyde is produced by the retinal pigment epithelium (RPE). However, in frog skin [9], bird hypothalamus [17], mammalian smooth muscle [53, 54], and mammalian skin, opsins must receive the retinaldehyde from an alternate source. In culture systems, exogenous retinaldehyde is often required [12, 28, 29, 54]. It will be of interest to determine the source and processing machinery for the proper chromophore function in these extra-ocular sites. Recent reports have demonstrated that the exposure of skin to short-wavelength light produces diverse systemic effects such as β-endorphin and urocanic acid production [55, 56]. The photoreceptors for these important effects have not been identified. The current work suggests OPN5 could be a candidate photopigment in skin for mediating diverse light-dependent physiologies.

STAR Methods

Lead Contact and Materials Availability

Additional information and any requests for reagents or mouse strains can be directed to and will be fulfilled by the Lead Contact, Ethan Buhr (buhre@uw.edu).

This study did not generate new unique reagents.

Experimental Model and Subject Details

Mice.—All animal experiments were carried out according to protocols approved by the Institutional Animal Care and Use Committee at the University of Washington and

Cincinnati Children's Hospital Medical Center. *Opn5*$^{-/-}$ mice were generated as described in [19]. *Opn5*^{Cre} mice were generated in-house at CCHMC transgenic core using CRISPR-Cas9 targeting. See allele design for details (Figure S1). Four guide RNAs that target exon 1 of *Opn5* were selected to knock in the *Cre* cassette. Plasmids containing the gRNA sequence were transfected into MK4 cells (an in-house mouse cell line representing induced metanephric mesenchyme undergoing epithelial conversion). The editing efficiency of gRNA was determined by T7E1 assay using PCR product-transfected MK4 cells. The sequence of the gRNA that was subsequently used for the transfection is TGGAGTCCTACTCGCGGACG. Sanger sequencing was performed to validate the knock-in sequence of founder mice. Primer sequences for genotyping the *Opn5*^{cre} allele are: Opn5cre-inF1: TGGAAAGAGATGCATTTGTGAG, Opn5cre-inR1: ACAGCCTATGAATTCTCTCAATGC and Opn5cre-inF2: CACTGCATTCTAGTTGTGGTTTGTCC. Primer pair Opn5cre-inF1/Opn5cre-inR1 detects wild type allele (300bp) and Opn5cre-inF2/ Opn5cre-inR1 detects cre allele (209 bp). Founder *Opn5*^{Cre} mice were bred to B6;129S6-*Gt(ROSA)26Sortm14(CAG-tdTomato)Hze*/J mice (JAX stock number 007908) to generate *Opn5*^{Cre}*; Ai14 tdTomato* animals. *Per2*^{Luciferase} PER2::LUCIFERASE fusion reporter mice were as reported in [1].

For immunohistochemistry, mice at postnatal day 8 were used as neonatal mice, and mice older than 6 weeks but younger than 1 year were used as adults.

For behavioral studies, *in vivo* studies of gene expression, and *ex vivo* tissue culture, mice older than 6 weeks but younger than one year were used.

For behavioral free-running of of *Opn4*$^{-/-}$*; Pde6b*$^{rd1/rd1}$ mice, mice were between 4 to 6 months old at the start of each experiment.

In all experiments care was taken to use both male and female mice. Mice were allowed access to food and water *ad libitum*, and were maintained in standard humidity with room temperature between 20°C and 25°C. Mice were randomly assigned to experimental groups based on their genotypes.

Method Details

Immunohistochemistry.—Animals were euthanized, and skin harvested at the indicated age. Tissues were fixed in 4% PFA at room temperature for two hours followed by two 15-minute washes in 1x PBS. Skin was cryoprotected in 30% sucrose solution in PBS, embedded in OCT (TissueTek) and sectioned at 16 μm. Slides were subjected to antigen retrieval in ice cold 10mM sodium citrate with 0.05% Tween-20 for 10 minutes. Subsequently, sections were blocked in 10% donkey serum with 0.5% Triton in 1x PBS and stained with antibodies to c-KIT (1:250, CellSignaling #mAb3074), MITF (1:250, Abcam # ab12039), DCT (1:250, Proteintech #13095-1-ap), LEF1 (1:500, Cell Signaling #2230S), and β-catenin (1:500, Santa Cruz Biotechnology #sc-7199) overnight at 4°C. Following three 15-minute washes in 1x PBS, secondary antibody (1:1000 Alexa 488 donkey anti-rabbit, 1:1000 Alexa 647 donkey anti-mouse, or 1:1000 Alexa 647 goat anti-rabbit) and Hoeschst 33342 labelling was performed at room temperature for one hour. Imaging was done on a Zeiss LSM 700 confocal microscope.

***Ex vivo* photoentrainment and light-induced gene expression.—**Animals were euthanized by CO_2 asphyxiation, and the skin was harvested and sterilized on the epidermal side with 70% isopropyl alcohol swabs before being placed into cold Hank's Balanced Salt Solution (HBSS, Thermo Fisher). Outer ears (pinna) were dissected along the cartilage layer by pulling apart the dermal layers on either side of the cartilage layer. Mystacial vibrissae pads were collected and 3 adjacent macrovibrissae were dissected including surrounding fat and muscle down to the base of the follicles. All skin explants were placed epidermal-side-up on cell-culture inserts (PICM0RG50, Millipore). Pituitary and liver samples were placed immediately onto cell culture inserts. Cell culture media consisted of Dulbecco's Modified Eagle Medium (DMEM) supplemented with B-27 supplement (Thermo Fisher), 352.5 μg/ml $NaHCO_3$, 10 mM HEPES (Thermo Fisher), 25 units/ml penicillin; 25 μg/ml streptomycin (Thermo Fisher), 0.1 mM luciferin potassium salt (Biosynth) and 10 μM 9-*cis* retinaldehyde (Sigma) or 10 μM *all-trans* retinaldehyde (Sigma) where noted. Organotypic cultures were sealed with vacuum grease and maintained in 36°C incubators without CO_2.

Light-dark cycles were administered to cultured tissue using a device which allows tissues at diametrically-opposed positions (designated 0° and 180°) to experience oppositely phased light-dark cycles as has been described previously [27]. Briefly, a motor drove a solid black disk with a pie-shaped transparent window at 24 h revolution such that each of the paired tissues was illuminated for 9 hours in every 24-h cycle. Light came from LEDs with peak wavelengths at 415 nm, 475 nm, and 530 nm. A Macam Q203 quantum radiometer was used for radiometric light measurements.

After 5 days of light-dark cycles, the cultured tissues were placed in constant darkness in a Lumicycle luminometer (Actimetrics), in which bioluminescence was measured continuously. Bioluminescence data were de-trended by using a polynomial fit with an order of 1 to remove the steady decline of background bioluminescence. To measure the period of oscillations, a best-fit sine-wave was fit to the detrended data (Lumicycle Analysis). Phases were determined using at least three days of oscillations.

For acute light-induction and phase shift experiments, the phase of a cultured tissue was measured using the second peak of luminescence compared to non-light treated control tissue as a guide within the Lumicycle machine. Tissue was then transferred in a light-proof, insulated chamber (to maintain constant culture temperature) to an incubator with 415 nm light at 5 W/m^2 for 90 minutes. Tissues were then placed in ice cold RNAlater (Qiagen) for later RNA extraction or monitored for luciferase expression rhythms. Phase delays are measured as expected minus observed $Per2^{Luciferase}$ rhythms after the light pulse, based on the phase and period of the rhythm before the light pulse. For the action spectrum, irradiance response curves for individual wavelengths were fit using a 4 parameter sigmoid curve with a Hill slope. Half-maximum values of these curves were then normalized to 1 for comparison with published absorption spectra.

For *in vivo* light-induction experiments, mice were entrained to a 12 h light: 12 h dark cycles for at least 3 weeks and then lights were turned off for 2 days of constant darkness. At the time corresponding to one hour past the onset of darkness (CT13) of the previous light-dark

cycle, mice were exposed to 415 nm light at 2 W/m^2 for 60 minutes before being euthanized by cervical dislocation and ears were dissected into cold RNAlater.

Imaging of bioluminescence *ex vivo*.—A custom darkbox was created to allow a Retiga Lumo CCD camera (Q-imaging) to image cultured tissue from beneath. Tissue was maintained at 36°C using a microscope stage incubator (Bioscience Tools). Luminescence was collected at 30 minute intervals to generate one image for a total of 48 images/day.

Analysis of *in vivo* clock gene transcription.—*Opn4*$^{-/-}$*; Pde6b*$^{rd1/rd1}$ mice were housed in cages equipped with running wheels. Wheel-running behavior was monitored continuously and recorded using ClockLab software (Actimetrics). Lights used included LEDs with peak spectral output at 415 nm (4.2 x 10^{14} photons cm^{-2} s^{-1}) and 475 nm (7.2 x 10^{14} photons cm^{-2} s^{-1}). After at least 3 weeks of exposure to the LD cycle, when behavioral onset of activity coincided with either lights-on or lights-off mice were euthanized using cervical dislocation and tissues were dissected under dim red light and stored in cold RNAlater. Animals were between 3 and 12 months of age and included both male and female mice. For analysis of clock gene expression in wild-type and *Opn5*$^{-/-}$ mice (Figure 3), mice were housed in cages as described above for a least 3 weeks before either being euthanized using cervical dislocation at specific clock times or placed in constant darkness for at least 36 hours before tissue collection.

RNA extraction and RT-PCR.—Total RNA was extracted from tissues using TRI-reagent (Thermo fisher) according to manufacturer's instructions, and cDNA was generated using High Capacity RNA to cDNA kit (Applied Biosystems). QPCR was performed using Absolute Blue QPCR mix (Thermo Fisher) on an Applied Biosystems 7500fast Real Time PCR machine. Relative quantities of transcripts were quantified using the $2^{\wedge}$-ΔΔCt method comparing the transcript of interest to *β actin* and comparing light treated groups to the dark control tissue from the same animal. Primer sequences are available in Supplemental Table 1.

For comparison of transcripts among tissue types in Figure 1, standard curve RT-PCR was used to avoid complications of differential expression of endogenous control genes between tissues. An amplicon for *Opn5* transcript was generated from cDNA from mouse retina and was cloned into a pCR 2.1 TOPO cloning vector (Life Technologies). Standard curves were generated using the *Opn5*-pCR 2.1 TOPO plasmid from 10^9 to 10^2 copies in a 1:100 dilution series.

Quantification and Statistical Analysis

For quantification of opsin transcript abundance in Figure 1J and Supplemental Figure 2, ANOVA was performed on the total data set and a Tukey post-hoc was run using Sigma Plot 11.0 software. N are reported in the figure legends. For *ex vivo* light induction of Figure 3A, transcript abundance was compared to the abundance of dark samples collected from the same cohort of animals. For *in vivo* separate animals were used for light and dark experiments. ANOVA was performed on the total data set and a Tukey post-hoc was run using Sigma Plot 11.0 software. N are reported in the figure legend. For the action spectrum

of Figure 3F, the N are as follows: **370 nm** light 10^{11} n = 5, 10^{12} n =6, $3x10^{12}$ n = 5, 10^{13} n = 5, 10^{14} n = 7, 10^{15} n = 5; **400 nm** light 10^{11} n = 4, 10^{12} n =6, $3x10^{12}$ n = 4, 10^{13} n = 5, 10^{14} n = 4, 10^{15} n = 4; **415 nm** light 10^{11} n = 4, 10^{12} n =5, $3x10^{12}$ n = 6, 10^{13} n = 7, 10^{14} n = 8, 10^{15} n = 7, 10^{16} n = 4; **475 nm** light 10^{13} n = 4, 10^{14} n =7, 10^{15} n = 4, 10^{16} n = 7, 10^{17} n = 7; **525 nm** light 10^{13} n = 5, 10^{14} n =7, 10^{15} n = 5, 10^{16} n = 6, 10^{17} n = 6. Sigmoid Hill curves with 4 parameters were fit to data from individual wavelengths using Sigma Plot 11.0. For Figure 4, ANOVA were run comparing both light conditions and genotype comparisons between WT and $Opn5^{-/-}$, and Tukey post-hoc tests were used. For Figure 5, ANOVA were run on data between groups for individual tissues and Tukey post-hoc tests were performed. N for Figures 4 and 5 are listed in the figure legends. For all quantified data mean ± SEM are shown. n represents individual animals for *in vivo* experiments and individual organotypic tissue cultures for *ex vivo* experiments.

Data and Code Availability

This paper did not generate any datasets or new code. All raw data is available upon request.

Supplementary Material

Refer to Web version on PubMed Central for supplementary material.

Acknowledgments

We would like to thank Denny Liggitt for his guidance in skin histology and helpful suggestions of antibody selection. This work was supported by NIH R01 GM124246 to EDB, R01 EY026921 to RVG, NIH P30EY001730, an unrestricted grant to the University of Washington Department of Ophthalmology from Research to Prevent Blindness, and the Mark J. Daily, MD Research Fund. This work was also supported by NIH grants R01 EY027077 and R01 EY027711 to RAL and by funds from the Goldman Chair of the Abrahamson Pediatric Eye Institute at Cincinnati Children's Hospital Medical Center.

References

1. Yoo SH, Yamazaki S, Lowrey PL, Shimomura K, Ko CH, Buhr ED, Siepka SM, Hong HK, Oh WJ, Yoo OJ, et al. (2004). PERIOD2::LUCIFERASE real-time reporting of circadian dynamics reveals persistent circadian oscillations in mouse peripheral tissues. Proc Natl Acad Sci U S A 101, 5339–5346. [PubMed: 14963227]
2. Yamazaki S, Numano R, Abe M, Hida A, Takahashi R, Ueda M, Block GD, Sakaki Y, Menaker M, and Tei H (2000). Resetting central and peripheral circadian oscillators in transgenic rats. Science 288, 682–685. [PubMed: 10784453]
3. Agrawal P, Houl JH, Gunawardhana KL, Liu T, Zhou J, Zoran MJ, and Hardin PE (2017). Drosophila CRY Entrains Clocks in Body Tissues to Light and Maintains Passive Membrane Properties in a Non-clock Body Tissue Independent of Light. Curr Biol 27, 2431–2441 e2433. [PubMed: 28781048]
4. Whitmore D, Foulkes NS, and Sassone-Corsi P (2000). Light acts directly on organs and cells in culture to set the vertebrate circadian clock. Nature 404, 87–91. [PubMed: 10716448]
5. Tanioka M, Yamada H, Doi M, Bando H, Yamaguchi Y, Nishigori C, and Okamura H (2009). Molecular clocks in mouse skin. J Invest Dermatol 129, 1225–1231. [PubMed: 19037239]
6. Kofuji P, Mure LS, Massman LJ, Purrier N, Panda S, and Engeland WC (2016). Intrinsically Photosensitive Retinal Ganglion Cells (ipRGCs) Are Necessary for Light Entrainment of Peripheral Clocks. PLoS One 11, e0168651. [PubMed: 27992553]

7. Cavallari N, Frigato E, Vallone D, Fröhlich N, Lopez-Olmeda JF, Foà A, Berti R, Sánchez-Vázquez FJ, Bertolucci C, and Foulkes NS (2011). A blind circadian clock in cavefish reveals that opsins mediate peripheral clock photoreception. PLoS Biol 9, e1001142. [PubMed: 21909239]
8. Ramirez MD, and Oakley TH (2015). Eye-independent, light-activated chromatophore expansion (LACE) and expression of phototransduction genes in the skin of Octopus bimaculoides. J Exp Biol 218, 1513–1520. [PubMed: 25994633]
9. Provencio I, Jiang G, De Grip WJ, Hayes WP, and Rollag MD (1998). Melanopsin: An opsin in melanophores, brain, and eye. Proc Natl Acad Sci U S A 95, 340–345. [PubMed: 9419377]
10. Regazzetti C, Sormani L, Debayle D, Bernerd F, Tulic MK, De Donatis GM, Chignon-Sicard B, Rocchi S, and Passeron T (2018). Melanocytes Sense Blue Light and Regulate Pigmentation through Opsin-3. J Invest Dermatol 138, 171–178. [PubMed: 28842328]
11. de Assis LVM, Moraes MN, Magalhães-Marques KK, and Castrucci AML (2018). Melanopsin and rhodopsin mediate UVA-induced immediate pigment darkening: Unravelling the photosensitive system of the skin. Eur J Cell Biol 97, 150–162. [PubMed: 29395480]
12. Rollag MD (1996). Amphibian melanophores become photosensitive when treated with retinal. Journal of Experimental Zoology 275, 20–26.
13. Rollag MD, Provencio I, Sugden D, and Green CB (2000). Cultured amphibian melanophores: a model system to study melanopsin photobiology. Methods Enzymol 316, 291–309. [PubMed: 10800682]
14. Becker HE, and Cone RA (1966). Light-stimulated electrical responses from skin. Science 154, 1051–1053. [PubMed: 5919759]
15. Yamashita T, Ohuchi H, Tomonari S, Ikeda K, Sakai K, and Shichida Y (2010). Opn5 is a UV-sensitive bistable pigment that couples with Gi subtype of G protein. Proc Natl Acad Sci U S A 107, 22084–22089. [PubMed: 21135214]
16. Kojima D, Mori S, Torii M, Wada A, Morishita R, and Fukada Y (2011). UV-sensitive photoreceptor protein OPN5 in humans and mice. PLoS One 6, e26388. [PubMed: 22043319]
17. Nakane Y, Ikegami K, Ono H, Yamamoto N, Yoshida S, Hirunagi K, Ebihara S, Kubo Y, and Yoshimura T (2010). A mammalian neural tissue opsin (Opsin 5) is a deep brain photoreceptor in birds. Proc Natl Acad Sci U S A 107, 15264–15268. [PubMed: 20679218]
18. Nakane Y, Shimmura T, Abe H, and Yoshimura T (2014). Intrinsic photosensitivity of a deep brain photoreceptor. Curr Biol 24, R596–597. [PubMed: 25004360]
19. Buhr ED, Yue WW, Ren X, Jiang Z, Liao HW, Mei X, Vemaraju S, Nguyen MT, Reed RR, Lang RA, et al. (2015). Neuropsin (OPN5)-mediated photoentrainment of local circadian oscillators in mammalian retina and cornea. Proc Natl Acad Sci U S A 112, 13093–13098. [PubMed: 26392540]
20. Lowry WE, Blanpain C, Nowak JA, Guasch G, Lewis L, and Fuchs E (2005). Defining the impact of beta-catenin/Tcf transactivation on epithelial stem cells. Genes Dev 19, 1596–1611. [PubMed: 15961525]
21. Petersson M, Brylka H, Kraus A, John S, Rappl G, Schettina P, and Niemann C (2011). TCF/Lef1 activity controls establishment of diverse stem and progenitor cell compartments in mouse epidermis. EMBO J 30, 3004–3018. [PubMed: 21694721]
22. Rahmani W, Abbasi S, Hagner A, Raharjo E, Kumar R, Hotta A, Magness S, Metzger D, and Biernaskie J (2014). Hair follicle dermal stem cells regenerate the dermal sheath, repopulate the dermal papilla, and modulate hair type. Dev Cell 31, 543–558. [PubMed: 25465495]
23. DasGupta R, and Fuchs E (1999). Multiple roles for activated LEF/TCF transcription complexes during hair follicle development and differentiation. Development 126, 4557–4568. [PubMed: 10498690]
24. Driskell RR, Giangreco A, Jensen KB, Mulder KW, and Watt FM (2009). Sox2-positive dermal papilla cells specify hair follicle type in mammalian epidermis. Development 136, 2815–2823. [PubMed: 19605494]
25. Seberg HE, Van Otterloo E, and Cornell RA (2017). Beyond MITF: Multiple transcription factors directly regulate the cellular phenotype in melanocytes and melanoma. Pigment Cell Melanoma Res 30, 454–466. [PubMed: 28649789]

26. de Assis LVM, Moraes MN, and Castrucci AML (2017). Heat shock antagonizes UVA-induced responses in murine melanocytes and melanoma cells: an unexpected interaction. Photochem Photobiol Sci 16, 633–648. [PubMed: 28203671]
27. Buhr ED, and Van Gelder RN (2014). Local photic entrainment of the retinal circadian oscillator in the absence of rods, cones, and melanopsin. Proc Natl Acad Sci U S A 111, 8625–8630. [PubMed: 24843129]
28. Sugiyama T, Suzuki H, and Takahashi T (2014). Light-induced rapid Ca(2+) response and MAPK phosphorylation in the cells heterologously expressing human OPN5. Sci Rep 4, 5352. [PubMed: 24941910]
29. Moldrup ML, Georg B, Falktoft B, Mortensen R, Hansen JL, and Fahrenkrug J (2010). Light induces Fos expression via extracellular signal-regulated kinases 1/2 in melanopsin-expressing PC12 cells. J Neurochem 112, 797–806. [PubMed: 19943848]
30. Yamashita T, Ono K, Ohuchi H, Yumoto A, Gotoh H, Tomonari S, Sakai K, Fujita H, Imamoto Y, Noji S, et al. (2014). Evolution of mammalian Opn5 as a specialized UV-absorbing pigment by a single amino acid mutation. J Biol Chem 289, 3991–4000. [PubMed: 24403072]
31. Shearman LP, Zylka MJ, Weaver DR, Kolakowski LF Jr., and Reppert SM (1997). Two period homologs: circadian expression and photic regulation in the suprachiasmatic nuclei. Neuron 19, 1261–1269. [PubMed: 9427249]
32. Shigeyoshi Y, Taguchi K, Yamamoto S, Takekida S, Yan L, Tei H, Moriya T, Shibata S, Loros JJ, Dunlap JC, et al. (1997). Light-induced resetting of a mammalian circadian clock is associated with rapid induction of the mPer1 transcript. Cell 91, 1043–1053. [PubMed: 9428526]
33. Albrecht U, Sun ZS, Eichele G, and Lee CC (1997). A differential response of two putative mammalian circadian regulators, mper1 and mper2, to light. Cell 91, 1055–1064. [PubMed: 9428527]
34. Daan S, and Pittendrigh CS (1976). A Functional Analysis of Circadian Pacemakers in Nocturnal Rodents II. The Variability of Phase Response Curves. J Comp Physiol A 106, 253–266.
35. Winfree AT (1970). Integrated view of resetting a circadian clock. J Theor Biol 28, 327–374. [PubMed: 5487648]
36. Plikus MV, Vollmers C, de la Cruz D, Chaix A, Ramos R, Panda S, and Chuong CM (2013). Local circadian clock gates cell cycle progression of transient amplifying cells during regenerative hair cycling. Proc Natl Acad Sci U S A 110, E2106–2115. [PubMed: 23690597]
37. Lin KK, Kumar V, Geyfman M, Chudova D, Ihler AT, Smyth P, Paus R, Takahashi JS, and Andersen B (2009). Circadian clock genes contribute to the regulation of hair follicle cycling. PLoS Genet 5, e1000573. [PubMed: 19629164]
38. Schibler U, Gotic I, Saini C, Gos P, Curie T, Emmenegger Y, Sinturel F, Gosselin P, Gerber A, Fleury-Olela F, et al. (2015). Clock-Talk: Interactions between Central and Peripheral Circadian Oscillators in Mammals. Cold Spring Harb Symp Quant Biol 80, 223–232. [PubMed: 26683231]
39. Husse J, Leliavski A, Tsang AH, Oster H, and Eichele G (2014). The light-dark cycle controls peripheral rhythmicity in mice with a genetically ablated suprachiasmatic nucleus clock. FASEB J 28, 4950–4960. [PubMed: 25063847]
40. Panda S, Provencio I, Tu DC, Pires SS, Rollag MD, Castrucci AM, Pletcher MT, Sato TK, Wiltshire T, Andahazy M, et al. (2003). Melanopsin is required for non-image-forming photic responses in blind mice. Science 301, 525–527. [PubMed: 12829787]
41. Tarttelin EE, Bellingham J, Hankins MW, Foster RG, and Lucas RJ (2003). Neuropsin (Opn5): a novel opsin identified in mammalian neural tissue. FEBS Lett 554, 410–416. [PubMed: 14623103]
42. Gaddameedhi S, Selby CP, Kaufmann WK, Smart RC, and Sancar A (2011). Control of skin cancer by the circadian rhythm. Proc Natl Acad Sci U S A 108, 18790–18795. [PubMed: 22025708]
43. Gaddameedhi S, Selby CP, Kemp MG, Ye R, and Sancar A (2015). The circadian clock controls sunburn apoptosis and erythema in mouse skin. J Invest Dermatol 135, 1119–1127. [PubMed: 25431853]
44. Geyfman M, Kumar V, Liu Q, Ruiz R, Gordon W, Espitia F, Cam E, Millar SE, Smyth P, Ihler A, et al. (2012). Brain and muscle Arnt-like protein-1 (BMAL1) controls circadian cell proliferation and susceptibility to UVB-induced DNA damage in the epidermis. Proc Natl Acad Sci U S A 109, 11758–11763. [PubMed: 22753467]

45. Spörl F, Korge S, Jürchott K, Wunderskirchner M, Schellenberg K, Heins S, Specht A, Stoll C, Klemz R, Maier B, et al. (2012). Krüppel-like factor 9 is a circadian transcription factor in human epidermis that controls proliferation of keratinocytes. Proc Natl Acad Sci U S A 109, 10903–10908. [PubMed: 22711835]

46. Hoyle NP, Seinkmane E, Putker M, Feeney KA, Krogager TP, Chesham JE, Bray LK, Thomas JM, Dunn K, Blaikley J, et al. (2017). Circadian actin dynamics drive rhythmic fibroblast mobilization during wound healing. Sci Transl Med 9.

47. Kowalska E, Ripperger JA, Hoegger DC, Bruegger P, Buch T, Birchler T, Mueller A, Albrecht U, Contaldo C, and Brown SA (2013). NONO couples the circadian clock to the cell cycle. Proc Natl Acad Sci U S A 110, 1592–1599. [PubMed: 23267082]

48. Kingston AC, and Cronin TW (2016). Diverse Distributions of Extraocular Opsins in Crustaceans, Cephalopods, and Fish. Integr Comp Biol 56, 820–833. [PubMed: 27252200]

49. Cahill GM, and Besharse JC (1991). Resetting the circadian clock in cultured Xenopus eyecups: regulation of retinal melatonin rhythms by light and D2 dopamine receptors. J Neurosci 11, 2959–2971. [PubMed: 1682423]

50. Ohuchi H, Yamashita T, Tomonari S, Fujita-Yanagibayashi S, Sakai K, Noji S, and Shichida Y (2012). A non-mammalian type opsin 5 functions dually in the photoreceptive and non-photoreceptive organs of birds. PLoS One 7, e31534. [PubMed: 22348098]

51. Wang H, van Spyk E, Liu Q, Geyfman M, Salmans ML, Kumar V, Ihler A, Li N, Takahashi JS, and Andersen B (2017). Time-Restricted Feeding Shifts the Skin Circadian Clock and Alters UVB-Induced DNA Damage. Cell Rep 20, 1061–1072. [PubMed: 28768192]

52. Stokkan KA, Yamazaki S, Tei H, Sakaki Y, and Menaker M (2001). Entrainment of the circadian clock in the liver by feeding. Science 291, 490–493. [PubMed: 11161204]

53. Sikka G, Hussmann GP, Pandey D, Cao S, Hori D, Park JT, Steppan J, Kim JH, Barodka V, Myers AC, et al. (2014). Melanopsin mediates light-dependent relaxation in blood vessels. Proc Natl Acad Sci U S A 111, 17977–17982. [PubMed: 25404319]

54. Yim PD, Gallos G, Perez-Zoghbi JF, Zhang Y, Xu D, Wu AD, Berkowitz DE, and Emala CW (2018). Airway smooth muscle photorelaxation via opsin receptor activation. Am J Physiol Lung Cell Mol Physiol.

55. Fell GL, Robinson KC, Mao J, Woolf CJ, and Fisher DE (2014). Skin β-endorphin mediates addiction to UV light. Cell 157, 1527–1534. [PubMed: 24949966]

56. Zhu H, Wang N, Yao L, Chen Q, Zhang R, Qian J, Hou Y, Guo W, Fan S, Liu S, et al. (2018). Moderate UV Exposure Enhances Learning and Memory by Promoting a Novel Glutamate Biosynthetic Pathway in the Brain. Cell 173, 1716–1727.e1717. [PubMed: 29779945]

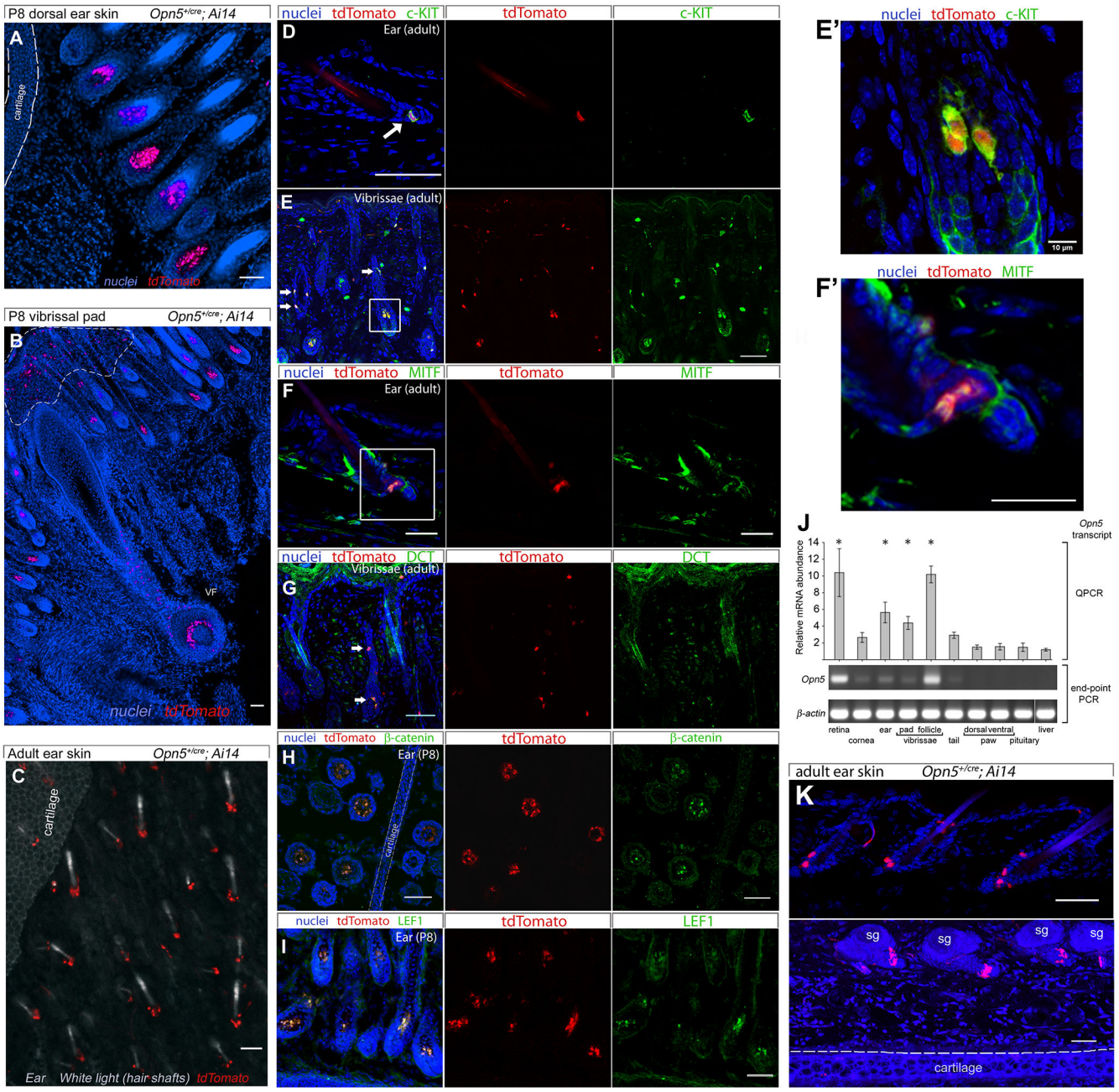

Figure 1. *Opn5* is expressed in LEF1 positive hair follicle stem cells.

(**A**, **B**) Overview images from labelled cryosections from P8 *Opn5*$^{+/cre}$*; Ai14* mice for dorsal ear skin (**A**) and P8 vibrissal pad skin (**B**). For these and all figure panels, blue shows nuclear labelling with Hoechst 33258 and red indicates expression of the *Ai14* tdTomato cre activity reporter. Clusters of tdTomato positive cells are observed in hair follicles (**A**, **B**) and in vibrissal follicle (**B**, VF). A sparsely distributed population of tdTomato positive cells is observed outside the follicles and closer to the skin surface (**B**, dashed white line). (**C**) td Tomato cell clusters (red) around bases of hair follicles in whole mount adult ear images with white light to visualize hair shafts. (**D-I**) In *Opn5*$^{+/cre}$*; Ai14* dorsal ear skin (**D, F, H-I**)

and vibrissal pad skin (**E, G**). tdTomato positive cells are also viewed with antibodies to c-KIT (**D** and **E**), MITF (**F**), DCT (**G**), β-Catenin (**H**, tranverse), and LEF1 (**I**). White arrows indicate strongly double-labeled cells or cell clusters. (**J**) *Opn5* transcript was detected in adult tissues using quantitative or end-point RT-PCR as labeled indicating active transcription of *Opn5* at this stage of development. All transcript levels as measured by standard curve qPCR are shown relative to expression in the liver. Retina, n=5; cornea, n=5; ear, n=5; vibrissal pad, n=5; vibrissal follicles, n=4; tail, n=4; paw, n=4; pituitary, n=5; liver, n=5. Bars represent means ± SEM. * $p < 0.05$, One Way ANOVA, Tukey post hoc. (**K**) Images from Hoechst 33258 labelled cryosections from adult *Opn5*$^{+/cre}$*; Ai14* mice for dorsal ear skin. sg, sebaceous glands. Scale bars represents 50μm unless otherwise noted. See also Figure S2.

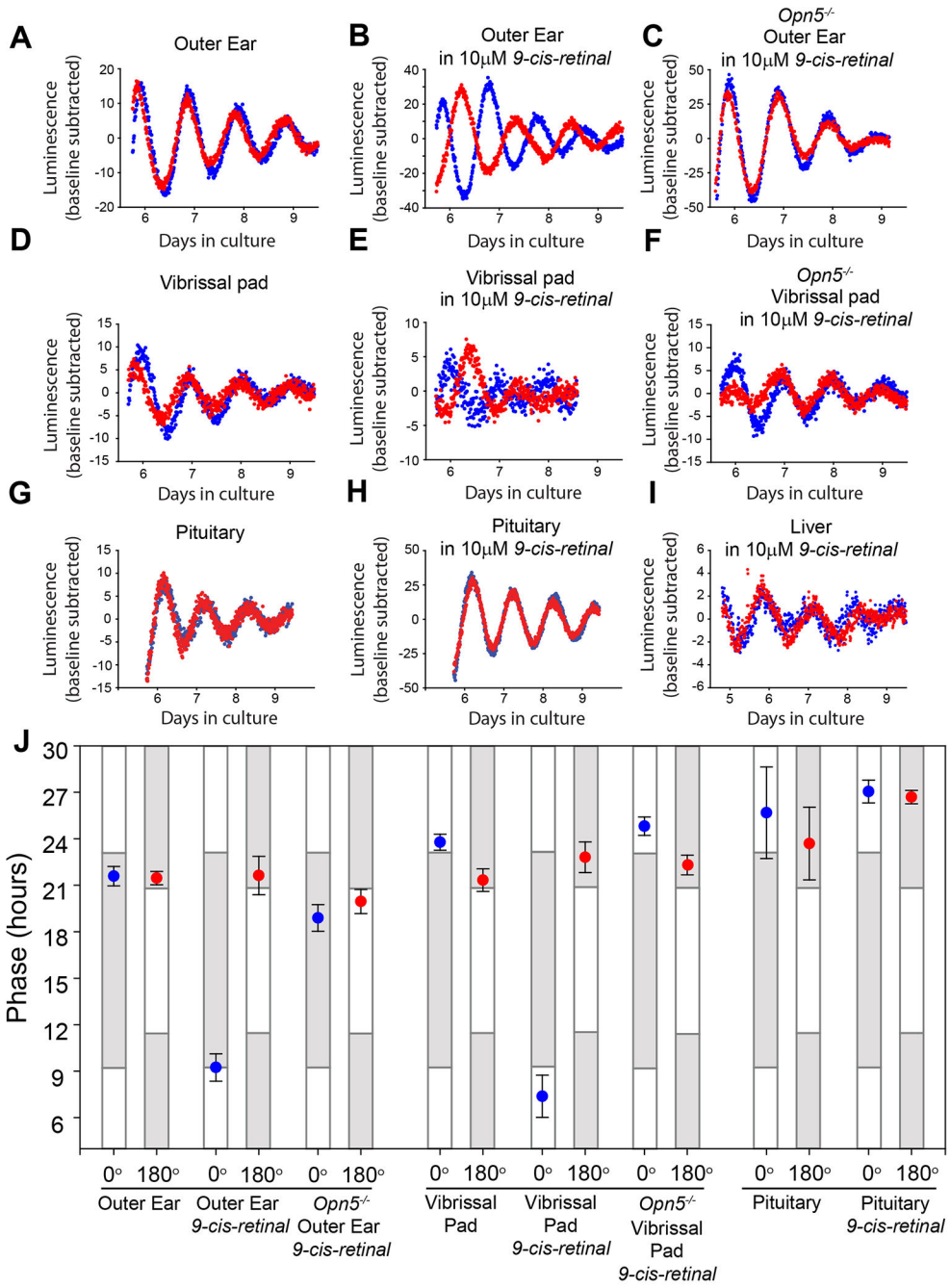

Figure 2. Cultures of outer ear and vibrissal pad exhibit OPN5-mediated photoentrainment.

Luminescence traces of cultured outer ear (pinna) from *Per2*^{Luc} mice after 5 days of an LD cycle *ex vivo* from wild-type mice without (**A**) or with (**B**) 10μM 9-*cis*-retinaldehyde, or from *Opn5*$^{-/-}$ mice with 10μM 9-*cis*-retinaldehyde (**C**). Blue and red traces represent two pieces of tissue from the same animal in independent culture dishes exposed to oppositely phased light-dark cycles. **D,E,F** The same as **A,B,C**, but vibrissal pad tissue. (**G**) Luminescence traces of pituitary (**G,H**) or liver (**I**) cultures after 5 days of an LD cycle *ex vivo*. (**J**) Phase of the peak of *Per2*^{Luc} luminescence on the day after 5 days of LD in either

the 0° or 180° position of a photoentrainment apparatus. Points show mean ± SEM. White and grey bars represent times at which the tissues experienced light or dark in the previous LD cycle. n = 5 pairs of cultures for each group. See also Figure S3.

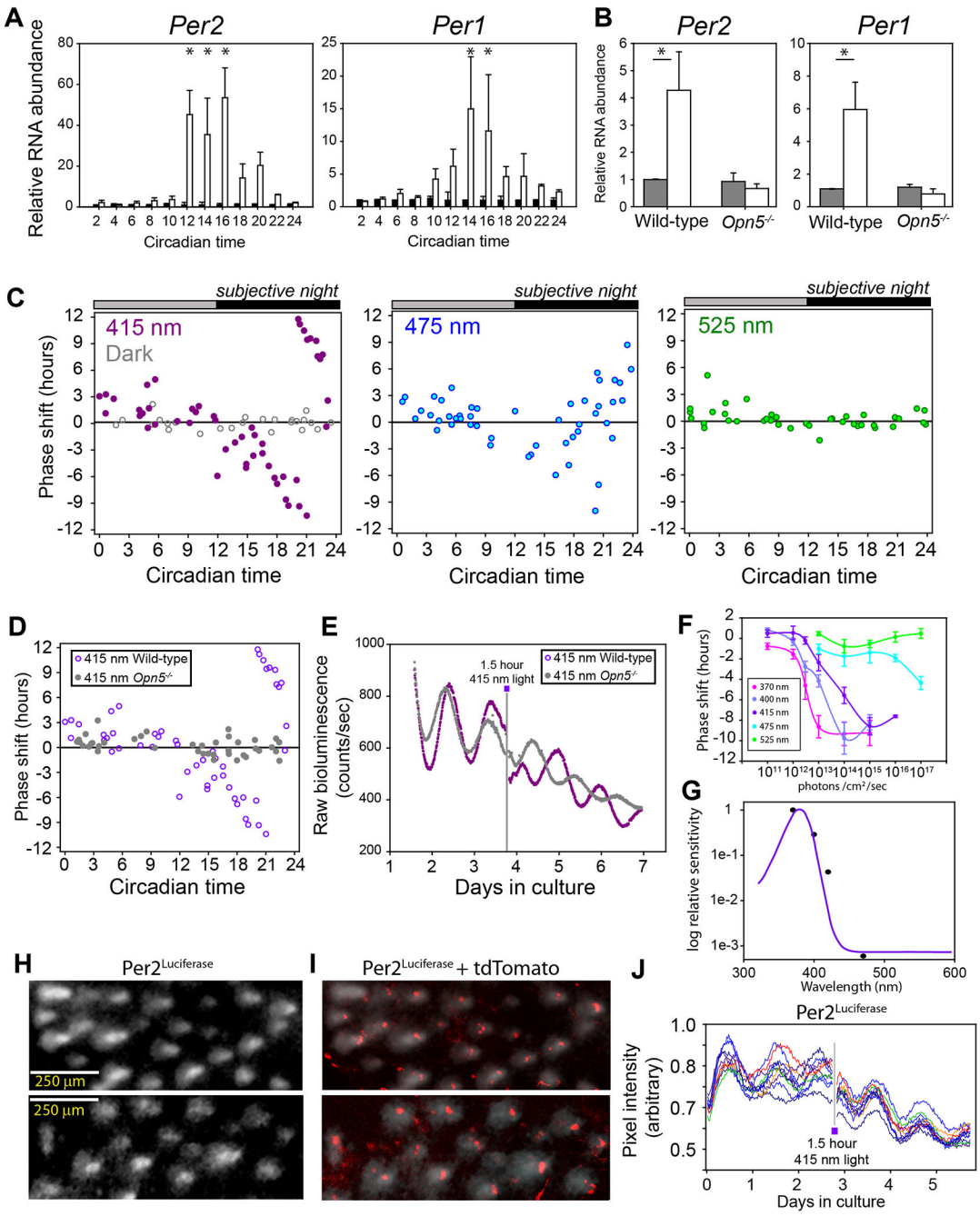

Figure 3. Induction of *Per* genes and phase shifts from acute light exposure.

(**A**) Relative RNA transcript from outer ear as measured by qPCR from wild-type organotypic tissue cultures. Tissues were cultured for 2 days and then given a 90 minute 5 W/m^2 violet light pulse beginning at the phase shown (white bars) or left in darkness (dark bars). All transcripts are shown relative to *β -actin* and relative to their own dark control (dark bars) using ΔΔCt RT-PCR. All tissues were incubated in 10 µM 9-*cis* retinaldehyde. (**B**) *Per2* and *Per1* induction in pinna skin of wild-type or *Opn5*$^{-/-}$ mice receiving a light pulse *in vivo*. Mice were entrained to an LD cycle and then placed in constant darkness for 2

days before receiving a 60 minute violet light pulse of $2W/m^2$ beginning at circadian time 13. **A** and **B** Two Way ANOVA $p < 0.05$. * = $p < 0.05$ in Tukey post-hoc analysis. CT2 n = 3, CT4 n = 3, CT6 n = 5, CT8 n = 5, CT10 n = 4, CT12 n = 4, CT14 n = 15, CT16 n = 4, CT18 n = 3, CT20 n = 3, CT22 n = 3, CT24 n = 3. In vivo, n=5 for dark groups, n = 7 for light groups. (**C**) Phase response curves of cultured *Per2*^{Luc} mouse pinnae receiving 90 minute, 2 x 10^{14} photons cm^{-2} s^{-1}, light pulses of 415 nm, 475 nm, or 525 nm. Handling controls performed in darkness shown as gray circles. Pulse times are shown as the beginning of the pulse in which circadian time 12 corresponds to the peak of *Per2*^{Luc} luminescence. (**D**) Phase response curve comparing wild-type (violet, same data as **C,** left) and *Opn5*$^{-/-}$ (gray) cultured pinnae. (**E**) Raw *Per2*^{luc} luminescence traces of wild-type (violet) or *Opn5*$^{-/-}$ (gray) pinnae receiving a 90 minute 415-nm light pulse on the third day where indicated. (**F**) Phase delays ellicted by a 90 minute light pulse of the indicated photic flux and wavelength. Points and error bars represent mean ± SEM. (**G**) Action spectrum of relative sensitivity of half maximum of data from **F** (black points) compared to mouse Opn5 absorbance spectrum (violet line) adapted from[16]. (**H**) *Per2*^{Luc} bioluminescence from a cultured mouse pinna as viewed from the base of hair follicles. (**I**) tdTomato expression (red) from *Opn5*$^{Cre/+}$*;Ai14* ear tissue overlayed with bioluminescence of *Per2*^{Luc} ear (white from **H**). (**J**) Quantification of individual bioluminescent hair follicles as in (**H**) imaged over 6 days. A 415 nm, 2 x 10^{14} photons cm^{-2} s^{-1} light pulse was given for 90 minutes on day 2.7 where noted. See also Video S1.

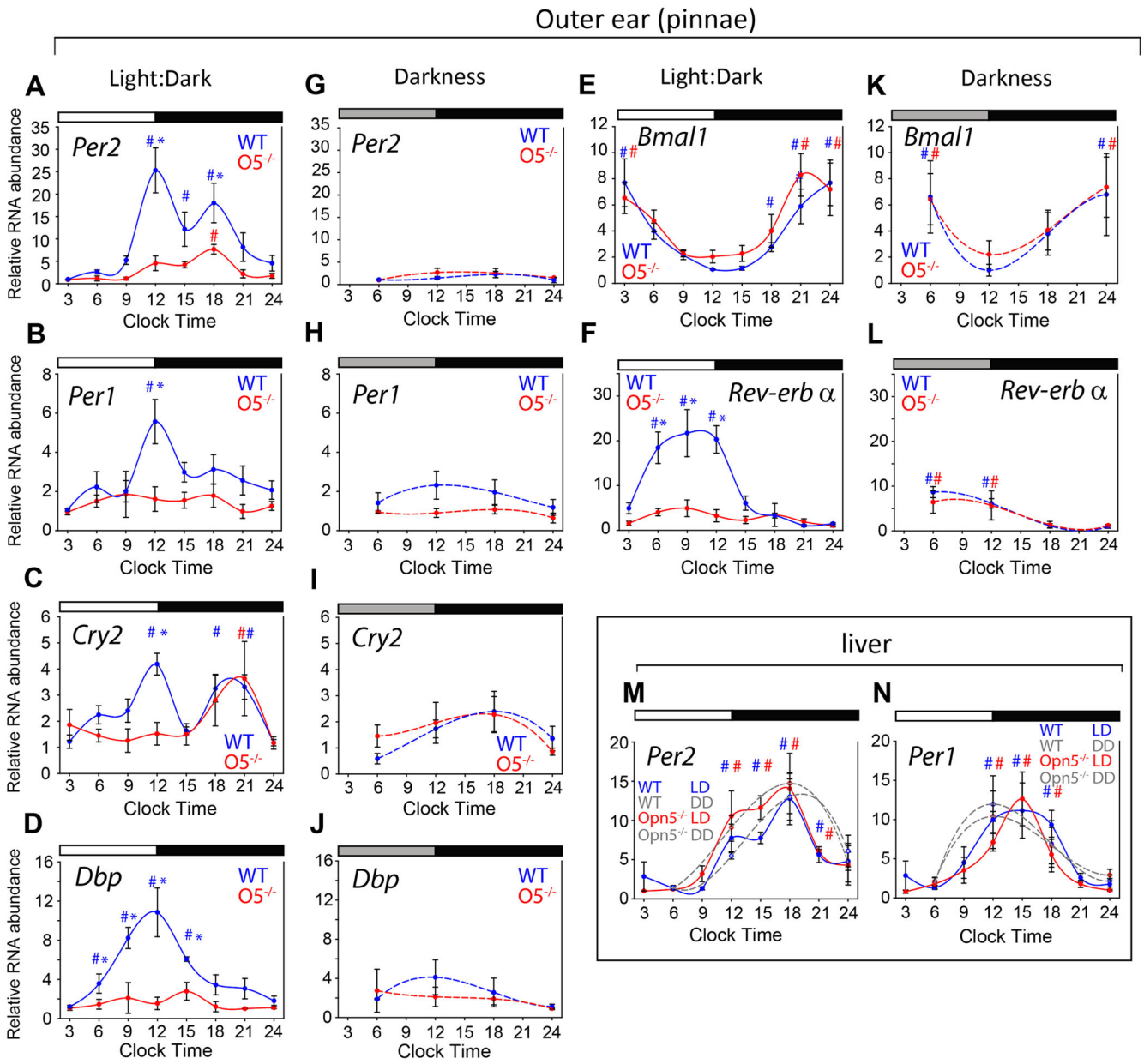

Figure 4. Expression of clock genes in wild-type and *Opn5*$^{-/-}$ outer ear.

Pinnae were harvested from mice that were housed in either a 12h:12h LD cycle (**A-F**) or in constant darkness for at least 36 hours (**G-L**). Transcript levels were determined using ΔΔCt RT-PCR. White and black boxes above charts indicate times of light or darkness in an LD cycle or the subjective LD cycle for groups in DD. Wild-type data are shown using blue symbols and data from *Opn5*$^{-/-}$ using red symbols. Charts (**M, N**) show data for liver from wild-type and *Opn5*$^{-/-}$, LD and DD as labeled. Each chart point indicates mean±SEM for n=4 in each group. To assess significant differences across a time-course, we used the ANOVA with Tukey post-hoc statistical test: $p < 0.05$ is indicated by the hash symbol (#). The same statistical test was used to assess difference between time-courses: $p < 0.05$ between groups is indicated by an asterisk (*). N = 4 mice for each point.

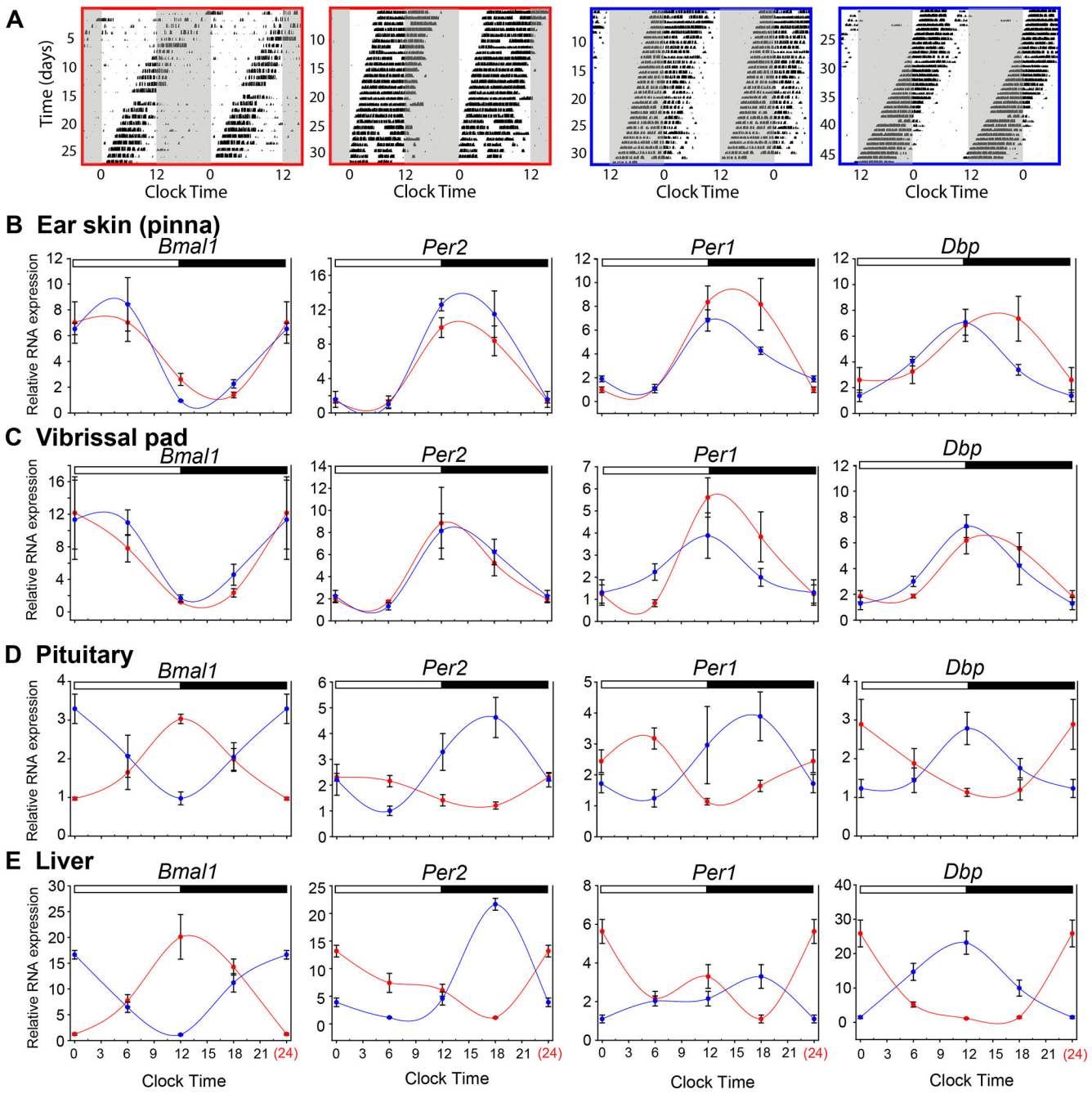

Figure 5. Circadian transcripts in the skin are entrained to LD cycles *in vivo*.

(**A**) Representative actograms of wheel-running behavior in *Opn4*$^{-/-}$; *Pde6b*$^{rd1/rd1}$ mice in a 12 hr light: 12 hr dark cycle. Actograms outlined in red show animals for which their behavioral onset coincides with lights-on on the last day shown. Actograms outlined in blue show mice in the opposite behavioral phase on the last day shown. (**B-E**) Transcript abundance from pinnae ear skin (**B**), vibrissal pad (**C**), pituitary (**D**), or liver (**E**) collected at clock times indicated based on the LD cycle. Traces in red indicate animals collected on the day when behavioral coincided with light onset. Traces in blue were collected from animals

when their behavioral onset coincided with dark onset. N = 4 mice for each point. Two way ANOVA results for **B**) non-significant p = 0.43 - 0.91; **C**) non-significant p = 0.16 – 0.70; **D**) p = 0.001 - 0.009, except *Dbp* p = 0.16; **E**) p = 0.001 – 0.043.

KEY RESOURCES TABLE

REAGENT or RESOURCE	SOURCE	IDENTIFIER
Antibodies		
c-KIT	Cell Signaling	Cat#mAb3074
MITF	Abcam	Cat#ab12039
DCT	Proteintech	Cat#13095-1-ap
LEF1	Cell Signaling	Cat#2230S
β-catenin	Santa Cruz	Cat#sc7199
Chemicals, Peptides, and Recombinant Proteins		
OCT	TissueTek	Cat#4583
Donkey serum	Jackson Immuno	Cat# 017-000121
Alexa Fluor 647 donkey anti mouse	Jackson Immuno	Cat#715-605-151
Alexa Fluor 647 goat anti-rabbit	Jackson Immuno	Cat#111-605-003
DMEM	Gibco	Cat#90-013-PB
B27 Supplement	Thermo Fisher	Cat#0080085SA
D-Luciferin potassium salt	Biosynth	Cat#L-8220
Hanks Balanced Salt Solution	Thermo Fisher	Cat#14025076
9-*cis*-retinaldehyde	Simga	Cat#R5754
all-trans-retinaldehyde	Sigma	Cat#R2500
RNAlater	Qiagen	Cat#76104
Tri reagent	Thermo Fisher	Cat#AM9738
Critical Commercial Assays		
High Capacity RNA to cDNA kit	Applied Biosystems	Cat#4387406
Absolute Blue QPCR mix	Thermo Fisher	Cat#AB4163A
Experimental Models: Organisms/Strains		
Period2::Luciferase, B6.129S6-*Per2*^{tm1Jt}/J	Jackson Laboratories	Stock# 006852
Opn5$^{-/-}$	[19]	N/A
Opn5^{Cre}*; Ai14*	[57]	N/A
B6;129S6-*Gt(ROSA)26Sortm14(CAG-tdTomato)*	Jackson Laboratories	Stock#007908
Opn4$^{-/-}$*;Pde6b*$^{rd1/rd1}$	[27]	N/A
Oligonucleotides		
Primers for circadian genes see Table S1	This paper	N/A
Primers for opsins see Table S1	This paper	N/A
Software and Algorithms		
ClockLab	Actimetrics	https://www.actimetrics.com/products/clocklab/
Lumicycle Analysis	Actimetrics	https://www.actimetrics.com/products/lumicycle/lumicycle-32/
ImageJ	NIH	https://imagej.nih.gov/ij/
Sigma Plot 11.0	Systat	systatsoftware.com
Other		

REAGENT or RESOURCE	SOURCE	IDENTIFIER
Zeiss LSM 700 confocal microscope	Zeiss	LSM 700
Abi7500 Fast Real-time PCR machine	Abi	7500 Fast
Quantum radiometer	Macam	Q203
Lumicycle luminometer	Actimeterics	Lumicycle 32
Retiga Lumo CCD camera	Q-imaging	Retiga Lumo
Microscope stage incubator	Bioscience tools	Cat#TC-MWPHB
Millicell cell culture inserts	Millipore	Cat#PICMORG50